Received: 28 January 2022 | Revised: 10 May 2022 | Accepted: 13 June 2022

DOI: 10.4218/etrij.2022-0036

ORIGINAL ARTICLE

ETRI Journal WILEY

An improved sparsity-aware normalized least-mean-square scheme for underwater communication

Anand Kumar | **Prashant Kumar**

Department of Electronics and Communication Engineering, National Institute of Technology Jamshedpur, Jamshedpur, India

Correspondence
Anand Kumar and Prashant Kumar, Department of Electronics and Communication Engineering, National Institute of Technology Jamshedpur, India.
Email: 2019rsec012@nitjsr.ac.in and prashant.ece@nitjsr.ac.in

Funding information
Science and Engineering Research Board (SERB), Department of Science & Technology (DST), Government of India, vide file no. SRG/2020/002486.

Abstract

Underwater communication (UWC) is widely used in coastal surveillance and early warning systems. Precise channel estimation is vital for efficient and reliable UWC. The sparse direct-adaptive filtering algorithms have become popular in UWC. Herein, we present an improved adaptive convex-combination method for the identification of sparse structures using a reweighted normalized least-mean-square (RNLMS) algorithm. Moreover, to make RNLMS algorithm independent of the reweighted l_1-norm parameter, a modified sparsity-aware adaptive zero-attracting RNLMS (AZA-RNLMS) algorithm is introduced to ensure accurate modeling. In addition, we present a quantitative analysis of this algorithm to evaluate the convergence speed and accuracy. Furthermore, we derive an excess mean-square-error expression that proves that the AZA-RNLMS algorithm performs better for the harsh underwater channel. The measured data from the experimental channel of SPACE08 is used for simulation, and results are presented to verify the performance of the proposed algorithm. The simulation results confirm that the proposed algorithm for underwater channel estimation performs better than the earlier schemes.

KEYWORDS
adaptive filtering, channel estimation, convergence speed, excess mean-square-error, reweighted NLMS, sparsity, underwater acoustics communication

1 | INTRODUCTION

Underwater acoustics (UWA) communication is widely used in fields such as marine intelligence, coastal surveillance, oil reconnaissance, pollution monitoring, and early warning systems. The design and implementation of efficient and reliable MODEM for UWA communication demand a comprehensive digital communication scheme. UWA propagation suffers from multipath fading and poor channel conditions [1, 2]. In such a scenario, precise channel estimation becomes very important. For the popular coherent UWA communication, a direct-adaptive equalizer (DAE) is often used, assisted by the least-mean-squares (LMS) [3] or recursive least square (RLS) [4] adaptive filter algorithms. With the growing complexity of the equalizer, standard DAEs face significant convergence and efficiency challenges. Moreover, the UWA channel consists of a sparse structure that concentrates significant energy of the channel impulse response (CIR) in a small fraction of its length [5]. Thus, sparse adaptive filters are encountered in various system identification problems, which has led to renewed interest in sparse

DAE research and modified sparse adaptive filtering techniques [4, 6, 7].

Whenever a need exists to normalize the step vector in terms of the input signal, a normalized LMS (NLMS) is generated. Unlike other parameter-estimation methods such as the RLS [6] and Kalman filters [8, 9], an impressive aspect of the NLMS algorithm is that it does not require significant stochastic knowledge of the channel and the input signal. However, as the parameter space increases, system-identification-related concerns become more tedious. For example, in combination with nonlinear acoustic cancelation of echoes, these structures may be found, where the global system resembles the Hammerstein model [10]. In addition to the sparse underwater channel, the transmitted acoustic signal also suffers from multipath fading [11].

In NLMS, the step size is used to normalize l_2-norm of the input signal vector in LMS with substantial fluctuation [12]. Numerous sparse algorithms for adaptive filters, such as proportionate NLMS (PNLMS) algorithms [11] and the zero-attracting (ZA) algorithm [13, 14], have been proposed to exploit this sparsity. The reweighted l_1-norm algorithm, which is more sensitive to input signal scaling, was introduced in the LMS cost function, resulting in ZA LMS [15, 16]. Furthermore, Tian et al. [3] evaluate some standard LMS algorithms, such as the l_0-norm and l_1-norm [17–19], and compare them experimentally with a UWA communication system. A channel estimation-based DAE produced experimental results in a practical underwater channel over a duration of five hours, which were presented and analyzed in an investigation of sparsity exploitation behavior with respect to UWA communication. Moreover, Tian and others [20] developed an improved LMS/fourth DAE (LMS/F-DAE) for the Arctic ice zone. The adaptive filtering algorithm has been introduced to minimize the logarithmic cost function of first- and second-order techniques, which is the logarithmic cost LMS and logarithmic cost RLS, resulting in a trade-off between convergence rate and steady-state performance [21].

To exploit the inherent sparsity characteristics of the multipath channel and reduce the computational complexity, sparsity-based LMS and NLMS algorithms have been designed to provide norms that are driven by compressed sensing (CS) techniques [22] in the cost function of the respective adaptive algorithms. The sparsity-aware reweighted l_1-norm constraint NLMS (RNLMS) algorithm was introduced by Al-Shabili and others [23]. Recently, the NLMS-based ZA and set-membership adaptive algorithm was presented and is employed to minimize computational complexity by exploiting the sparsity [24]. Similar research on set-membership NLMS (SM-NLMS) methods has been done to develop reweighted ZA set-membership NLMS and ZA set-membership NLMS algorithms from the ZA and RZA methods [25, 26]. Therefore, an improved channel estimation performance of NLMS and its variants with reweighted ZA set-membership NLMS and ZA set-membership NLMS algorithms have been proposed. Furthermore, by using the system sparsity, various sparsity-aware normalized least mean absolute third (NLMAT) algorithms were introduced [27] by mixing the conventional NLMAT algorithm with a penalty for promoting sparsity that assigns an upper bound to the square error. Moreover, as part of the sparse-signal-recovery–driven framework, the sparsity-promoting LMS and NLMS (SNLMS) algorithms use $\gamma_1 = 0$, where γ_1 is the regularization parameter, to reinforce sparsity without introducing bias in the adaptation process [28]. In Pelekanakis and Chitre [7, 29], the improved-proportionate NLMS (IPNLMS) algorithm with l_0-norm regularization has been introduced where the scheme is demonstrated by the estimating a mobile UWA channel. To exploit the sparsity feature of the UWA channel, we present a correntropy-induced metric CIM-penalized SM-proportionate NLMS method [30]. The UWA channel estimation behavior is investigated to explore the CIM-penalized SM-proportionate NLMS algorithm in detail. Recently, for underwater channel estimation, practical investigations have been undertaken of the sparse method, known as the nonuniform norm constraint LMS algorithm and that incorporates the nonuniform norm constraint into the conventional LMS cost function according to the absolute value of the individual coefficient [17].

1.1 | Motivation and contribution

The sparse underwater channel structure can be modified to provide a better estimation of the channel in the generic algorithms. The sparse-aware algorithm seeks to optimize the convergence speed and the steady-state mean-square-error (MSE) [31, 32]. An $N \times N$ orthogonal matrix can also be used and represent a different sparsity context [16]. NLMS algorithm usually converges more quickly than the LMS algorithm because the former uses the variable convergence factor to minimize instantaneous output failure with the NLMS method [22, 28]. CS algorithms have been introduced for the relative delay estimate from the minimum eigenvalue estimated by log-sum penalized minor component analysis [33]. Moreover, the penalty for the reuse of data is increased by a misadjustment procedure, where the usual compromise between ultimate misadjustment and a convergence factor is established [10].

The algorithm proposed herein exploits the sparseness of underwater multipath channels. As shown by the

detailed literature review, such an algorithm has not been proposed yet for underwater channel estimation. The technique is demonstrated by applying it to simulated data from the Surface Process Acoustic Communication Experiment (SPACE08) underwater channel.

This paper makes the following contribution:

1. It proposes the modified RNLMS algorithm, which is based on modifying the affine projection NLMS error function by adding the l_1-norm as a penalty term, also representing the CIR reweighting coefficient.
2. It introduces into the standard NLMS framework the adaptive zero-attraction RNLMS (AZA-RNLMS) algorithm based on a penalty term, resulting in faster convergence speed and better accuracy for underwater channels.
3. It derives the excess MSE (EMSE) and obtains convergence of the AZA-RNLMS algorithm applied to the sparse UWA channel.

The remainder of the paper is organized as follows: Section 2 presents the system model of the standard NLMS and RNLMS algorithms and the adaptive l_1-norm minimization parameter–based RNLMS algorithm. Section 3 presents a theoretical study of the convergence of the mean and the EMSE for the modified RNLMS algorithm. Section 4 presents the simulation results and compares the performance of the sparsity-aware NLMS and LMS algorithms in Gaussian and underwater channels. The underwater channel simulation and experimental channel data are used to verify the performance of the proposed method. Finally, Section 5 concludes the paper.

Notation

Bold symbols ($\mathbf{A}$) represent a set, a matrix, or a vector. $\mathbf{A}^{\mathrm{T}}$, $\|\mathbf{A}\|_1$, and Tr(A) are a matrix transpose, l_1-norm of the matrix, and matrix trace, respectively. $\mathbf{I}$ is the identity matrix.

2 | SYSTEM MODEL

The system design of UWA communication requires precise channel estimation.

2.1 | Underwater channel characteristics

The ability of adaptive signal processing algorithms, both with and without sparsity constraints, to monitor shallow-water channels in real time is limited by nonstationary variations in the channel delay spread caused by oceanographic fluctuations. The uncertainty principle, which dictates the localization of the nonstationary channel delay spread in time and frequency, must be extended to account for the fluctuating sparseness of the channel. Because of the uncertainty associated with sparsity across the transient delay taps, the direct use of sparse sensing techniques in the shallow-water domain is very challenging. This is especially true in moderate-to-rough seas [34].

2.2 | Standard NLMS algorithm

The NLMS algorithm supplements the standard LMS algorithm, which is used to estimate the actual CIR of the communication system. Figure 1 shows the system model of the adaptive identification problem, where the input vector $\mathbf{s}(k)$ is represented as $\mathbf{s}(k) \triangleq [s_k\ s_{k-1}\ \ldots\ s_{k-N+1}]^{\mathrm{T}}$, where k is the time index and N is channel length. The input vector $\boldsymbol{s}(k)$ is transmitted over an unknown finite impulse response channel $\mathbf{h} \triangleq [h_1\ h_2\ \ldots\ h_N]^{\mathrm{T}} \in N \times 1$ and $\mathbf{h}(k) \triangleq [h_{1,k}\ h_{2,k}\ \ldots\ h_{N,k}]^{\mathrm{T}}$ $N \times K$, and $\mathbf{y}(k) = \mathbf{s}^{\mathrm{T}}(k)\mathbf{h}(k)$ is the output of the multipath fading channel. The desired vector $\mathbf{d}(k)$ is known.

At the receiver, the desired signal $\mathbf{d}(k)$ is acquired and $\mathbf{d}(k) = \mathbf{s}^{\mathrm{T}}(k)\mathbf{h}(k) + \mathbf{n}(k)$, where the sparse CIR $\mathbf{h}(k)$, given $\mathbf{s}(k)$ and $\mathbf{d}(k)$, comes from the Wiener theory. Here, $\mathbf{n}(k)$ is the additive white Gaussian noise (AWGN). An error function associated with the estimation error $\mathbf{e}(k)$ is used to estimate the unknown finite impulse response sparse channel $\mathbf{h}(k)$ by using the conventional adaptive filtering techniques. According to the NLMS, the second-order estimated error $\mathbf{e}^2(k)$ is used in this calculation. The conventional NLMS channel estimation

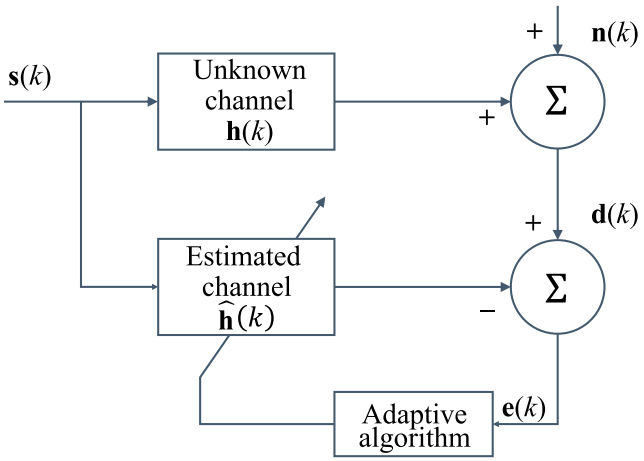

FIGURE 1 Block diagram of adaptive filter communication system

algorithm strives to minimize the instant error $\mathbf{e}(k)$ of the unknown sparse channel. The error signal is defined as $\mathbf{e}(k)=\mathbf{d}(k)-\mathbf{s}^{\mathrm{T}}(k)\hat{\mathbf{h}}(k)$, where $\hat{\mathbf{h}}(k)$ denotes the estimated vector and the error vector $\mathbf{e}(k)$ is defined as $\mathbf{e}(k)=[e_k\ e_{k-1}\ ...\ e_{k-N+1}]^{\mathrm{T}}$. The cost function of the conventional NLMS algorithm is

$$\begin{aligned}\min\ & \frac{1}{2}\|\hat{\mathbf{h}}(k+1)-\hat{\mathbf{h}}(k)\|^2\\ \text{s.t.}\ & \mathbf{d}(k)-\mathbf{s}^{\mathrm{T}}(k)\hat{\mathbf{h}}(k+1)=0.\end{aligned} \tag{1}$$

The Lagrange multiplier is used to solve this optimization problem [8]. Thus, the cost function of NLMS algorithm can be expressed as

$$\begin{aligned}\mathbf{J}(k)=\ & \frac{1}{2}\|\hat{\mathbf{h}}(k+1)-\hat{\mathbf{h}}(k)\|^2\\ & +\lambda[\mathbf{d}(k)-\mathbf{s}^{\mathrm{T}}(k)\hat{\mathbf{h}}(k+1)],\end{aligned} \tag{2}$$

where λ is the Lagrange multiplier, which is real-valued. Furthermore, we use a scaling factor $\mu>0$ to control the adaptation and a least regularization constant $\delta>0$ to avoid division by zero. Equation (2) is minimized by using the Lagrange multiplier method, and the conventional NLMS provides

$$\hat{\mathbf{h}}(k+1)=\hat{\mathbf{h}}(k)+\mu(k)\mathbf{e}(k)\mathbf{s}(k), \tag{3}$$

where $\mu(k)$ is the normalized step size of the NLMS algorithm, which takes the form $\mu(k)=\mu/(\mathbf{s}^{\mathrm{T}}(k)\mathbf{s}(k)+\delta)$, μ is the step size, and δ is a small value regularization parameter to avoid division by zero. For the NLMS convergence-analysis algorithm, the error coefficient vector is

$$\mathbf{v}(k)\triangleq\hat{\mathbf{h}}(k)-\mathbf{h}(k). \tag{4}$$

The input data vector $\mathbf{s}(k)$ is random and is an independent and identically distributed (i.i.d.) binary-phase-shift keying sequence that is independent of $\mathbf{v}(k)$, where $\mathbf{v}(k)\in N\times K$. In addition, the EMSE is calculated as

$$\xi(k)=\mathrm{E}[(\mathbf{v}^{\mathrm{T}}(k)\mathbf{s}(k))^2]=\mathrm{tr}\{\mathbf{R}\mathrm{E}[\mathbf{v}^{\mathrm{T}}(k)\mathbf{v}(k)]\}, \tag{5}$$

where the covariance matrix $\mathbf{R}$ is defined as the ensemble average of the input data vector $\mathbf{s}(k)$, which is $\mathbf{R}=\mathrm{E}[\mathbf{s}^{\mathrm{T}}(k)\mathbf{s}(k)]$.

Furthermore, the l_1-norm is used as a sparsity-promoting penalty, which results in the RNLMS method for sparse system estimation. This was inspired by the least absolute shrinkage and selection operator regression.

2.3 | Sparse RNLMS algorithm

The standard NLMS algorithm ensures that the cost function is convex such that, under the conditions mentioned earlier, the gradient descent algorithm converges to the optimum point in step size (μ). This paper considers the case of sparse CIRs. Furthermore, to improve underwater sparse-channel estimates, we propose to integrate a CIR reweighted l_1-norm as a sparsity penalty into the cost function of a conventional NLMS algorithm to use the sparse structure of UWA communication. The results show that nonconvex optimization leads to better sparsity than convex optimization [10]. The reweighted l_1-norm penalty is also known as CS.

The reweighted l_1-norm minimization for the sparse recovery of the signal is more effective than that used for the CS in the standard l_1-norm minimization [10]. The cost function of RNLMS is

$$\begin{aligned}j(k)=\ & \frac{1}{2}\|\hat{\mathbf{h}}(k+1)-\hat{\mathbf{h}}(k)\|^2\\ & +\lambda[\mathbf{d}(k)-\mathbf{s}^{\mathrm{T}}(k)\hat{\mathbf{h}}(k+1)]\\ & +\gamma_1\|\beta(k)\hat{\mathbf{h}}(k)\|_1,\end{aligned} \tag{6}$$

where γ_1 is the penalty term and $\beta(k)$ is the weight element with the penalty for the ith element of the $1\times N$ row vector that can be denoted

$$[\beta(k)]_i=\frac{1}{\varepsilon_1+[|\hat{\mathbf{h}}(k-1)|_i]};\ i=1,\ 2,\ 3,\ ...,\ N.$$

Equation (6) is minimized by using the Lagrange multiplier method, and the filter coefficient is updated in the RNLMS algorithm as

$$\hat{\mathbf{h}}(k+1)=\hat{\mathbf{h}}(k)+\mu(k)\mathbf{e}(k)\mathbf{s}(k)-\alpha_r\frac{\mathrm{sgn}(\hat{\mathbf{h}}(k))}{|\hat{\mathbf{h}}(k-1)|+\varepsilon_1}, \tag{7}$$

where $\mathrm{sgn}(\bullet)$ gives the sign of the arguments and operates separately on each vector element. The function $\mathrm{sgn}(\bullet)$ is defined as

$$\mathrm{sgn}(z)=\begin{cases}1 & \text{if } z>1\\ 0 & \text{if } z=0\\ -1 & \text{if } z<0,\end{cases} \tag{8}$$

where $\alpha_r=\mu(k)\gamma_1$. The last term of (7), the ith element of $\mathrm{sgn}(\hat{\mathbf{h}}(k))/(|\hat{\mathbf{h}}(k-1)|+\varepsilon_1)$, is $[\mathrm{sgn}(\hat{\mathbf{h}}(k))]_i/(|[\hat{\mathbf{h}}(k-1)]_i|+\varepsilon_1)$. The sparsity-aware NLMS algorithm changes with the weight vector and does not depend on $\mathbf{h}(k)$, and the cost function (6) is convex. The parameter $\varepsilon_1>0$ is set to ensure stability such that the zero value in $\hat{\mathbf{h}}(k)$ does not explicitly prohibit a nonzero estimate [35]. In addition, it

must ensure that a small positive value of ε_1 is less than the expected nonzero magnitude of $\hat{\mathbf{h}}(k)$.

2.4 | Proposed adaptive ZA-based RNLMS algorithm

Reweighted l_1-norm algorithms depend on the parameter α_r. Wang and others [18] eliminated the dependence of the proposed RNLMS algorithm on α_r by developing the AZA-RNLMS algorithm, which uses

$$\hat{\mathbf{h}}(k+1)=\hat{\mathbf{h}}(k)+\mu(k)\mathbf{e}(k)\mathbf{s}(k) -\alpha_{ar}(k+1)\frac{\operatorname{sgn}(\hat{\mathbf{h}}(k))}{|\hat{\mathbf{h}}(k-1)|+\varepsilon_1}, \tag{9}$$

where $\alpha_{ar}(k+1)$ is the adaptive l_1-norm minimization parameter, which is defined as

$$\alpha_{ar}(k+1)=\begin{cases}\dfrac{\Psi(k+1)-\mu(k)\Omega(k+1)}{\Phi(k+1)} & \text{if } \Phi(k+1)\neq 0\\ 0 & \text{if } \Phi(k+1)=0.\end{cases} \tag{10}$$

A new "smoothing" parameter $\nabla>0$ is introduced, which is greater than zero and close to unity to apply sufficient time smoothing. Thus, from (10),

$$\Psi(k+1)=\nabla\Psi(k)-(1-\nabla)\mathbf{v}(k)\|\hat{\mathbf{h}}(k)\|_0, \tag{11}$$

$$\Omega(k+1)=\nabla\Omega(k)-(1-\nabla)\mathbf{e}(k)\mathbf{s}^{\mathrm{T}}(k)\|\hat{\mathbf{h}}(k)\|_0, \tag{12}$$

$$\Phi(k+1)=\nabla\Phi(k)-(1-\nabla)\|\hat{\mathbf{h}}(k)\|_0^{\mathrm{T}}\|\hat{\mathbf{h}}(k)\|_0, \tag{13}$$

where $\Psi(k),\Omega(k)$, and $\Phi(k)$ are the instantaneous approximations of the terms $\mathrm{E}[\mathbf{v}(k)\|\hat{\mathbf{h}}(k)\|_0]$, $\mathrm{E}[\mathbf{e}(k)\mathbf{s}^{\mathrm{T}}(k)\|\hat{\mathbf{h}}(k)\|_0]$, and $\mathrm{E}[\|\hat{\mathbf{h}}(k)\|_0^{\mathrm{T}}\|\hat{\mathbf{h}}(k)\|_0]$, respectively. Initially, we select $\Psi(k)=0,\Omega(k)=0$, and $\Phi(k)=0$. Equation (10) shows that the l_1-norm reweighted parameter $\alpha_{ar}(k+1)$ depends on the next values of three parameters such as $\Psi(k+1),\Omega(k+1)$, and $\Phi(k+1)$, which are defined in (11)–(13), respectively, when $\Phi(k+1)\neq 0$. Otherwise, from (13), the term $\Phi(k+1)=0$, so $\alpha_{ar}(k+1)=0$ from (10), which means that $\hat{\mathbf{h}}(k+1)$ in (9) behave like a standard NLMS algorithm. It is therefore understood that $\Phi(k+1)$ determines the next value of α_{ar}. So, whenever $\alpha_{ar}(k+1)=0$, the proposed algorithm also becomes independent of the reweighted parameter, which is determined by $\Phi(k+1)$. Now, $\Phi(k+1)$ is decided by (13), which further depends upon the smoothing parameter ∇.

3 | ANALYSIS OF CONVERGENCE OF MSE WITH AZA-RNLMS ALGORITHM

We now analyze the AZA-RNLMS algorithm applied to a sparse underwater channel. The theoretical expression for the EMSE of the AZA-RNLMS algorithm is derived from considerations of energy conservation.

3.1 | Convergence of MSE

Let us consider the updated desired response $\mathbf{d}(k)$ that arises from the linear function and the estimated tap-weight vector $\hat{\mathbf{h}}$. To analyze the steady-state MSE of the proposed AZA-RNLMS algorithm, we define the following:

$$\mathrm{MSE}\equiv\lim_{k\to\infty}\mathrm{E}|\mathbf{v}(k)|^2. \tag{14}$$

Combining (4) and (7), the updated equation of the AZA-RNLMS algorithm can be written as

$$\mathbf{v}(k+1)=\left[\mathbf{I}-\frac{\mu\mathbf{s}(k)\mathbf{s}^{\mathrm{T}}(k)}{(\|\mathbf{s}(k)\|^2+\delta)}\right]\boldsymbol{v}(k)-\frac{\mu\mathbf{s}(k)\mathbf{n}(k)}{(\|\mathbf{s}(k)\|^2+\delta)} -\alpha_1\frac{\operatorname{sgn}(\hat{\mathbf{h}}(k))}{|\hat{\mathbf{h}}(k-1)|+\varepsilon_1}, \tag{15}$$

where $\alpha_1=\alpha_{ar}(k+1)$ and $\mathbf{n}(k)$ is the i.i.d Gaussian noise vector and is independent of $\mathbf{s}(k)$ because $\mathrm{E}[\mathbf{s}(k)\mathbf{n}(k)]=0$. Given that $\mathbf{v}^{\mathrm{T}}(k)\mathbf{s}(k)=\mathbf{s}^{\mathrm{T}}(k)\mathbf{v}(k)$ is a scalar quantity,

$$\mathrm{E}[\mathbf{v}(k+1)]=\mathrm{E}\left[\mathbf{I}-\frac{\mu\mathbf{s}(k)\mathbf{s}^{\mathrm{T}}(k)}{(\|\mathbf{s}(k)\|^2+\delta)}\right]\mathbf{v}(k) -\mathrm{E}\left[\frac{\mu\mathbf{s}(k)\mathbf{n}(k)}{(\|\mathbf{s}(k)\|^2+\delta)}\right]-\mathrm{E}\left[\alpha_1\frac{\operatorname{sgn}(\hat{\mathbf{h}}(k))}{|\hat{\mathbf{h}}(k-1)|+\varepsilon_1}\right]. \tag{16}$$

For a large signal-to-noise ratio (SNR) and a small α_1, a steady-state solution is assumed:

$$\mathrm{E}[\operatorname{sgn}(\hat{\mathbf{h}}(k)]\approx\operatorname{sgn}(\mathbf{h}). \tag{17}$$

For a significant value of the filter,

$$\mathrm{E}\left[\frac{\mathbf{s}(k)\mathbf{s}^{\mathrm{T}}(k)}{\|\mathbf{s}(k)\|+\delta}\right] \approx \frac{\mathrm{E}[\mathbf{s}(k)\mathbf{s}^{\mathrm{T}}(k)]}{\mathrm{E}[\|\mathbf{s}(k)\|+\delta]} = \frac{\mathbf{R}}{\mathrm{tr}(R)+\delta} = \frac{\mathbf{R}}{N\sigma_s^2+\delta}, \tag{18}$$

where σ_s^2 is the power of the input signal $\mathbf{s}(k)$. Equation (16) can then be written as

$$\mathrm{E}[\mathbf{v}(k+1)] = \left[\mathbf{I}-\frac{\mu\mathbf{R}}{(N\sigma_s^2+\delta)}\right]\mathrm{E}[\mathbf{v}(k)] - \mathrm{E}\left[\alpha_1\frac{\mathrm{sgn}(\hat{\mathbf{h}}(k))}{|\hat{\mathbf{h}}(k-1)|+\varepsilon_1}\right]. \tag{19}$$

The expression $\mathrm{sgn}(\hat{\mathbf{h}}(k))/(|\hat{\mathbf{h}}(k-1)|+\varepsilon_1)$ is bounded as follows:

$$-\frac{\mathbf{I}}{\varepsilon_1} \le \frac{\mathrm{sgn}(\hat{\mathbf{h}}(k))}{|\hat{\mathbf{h}}(k-1)|+\varepsilon_1} \le \frac{\mathbf{I}}{\varepsilon_1}, \tag{20}$$

where $\mathbf{I}$ is an identity vector whose entries are all set to unity. Consequently, ε_1 and $|\hat{\mathbf{h}}(k-1)|$ are nonnegative at every time index; that is, $|\hat{\mathbf{h}}(k-1)|+\varepsilon_1 \ge \varepsilon_1$, implying that (20) is always valid. Furthermore, we based on (19), and we see that, between $-(\alpha_1/\varepsilon_1)\mathbf{I}$ and $(\alpha_1/\varepsilon_1)\mathbf{I}$, $\alpha_1\mathrm{E}\left[\mathrm{sgn}(\hat{\mathbf{h}}(k))/(|\hat{\mathbf{h}}(k-1)|+\varepsilon_1)\right]$ is valid. We use the upper bound of (20) to study the mean convergence of the AZA-RNLMS algorithm.

The parameters depend only on the previous input signal vector. However, in the second presumption, the error signal at the optimal solution is orthogonal to the elements of the signal vector. Let $\mathbf{Q}$ be the unitary matrix and premultiply (19) by $\mathbf{Q}^{\mathrm{T}}$, which diagonalizes $\mathbf{R}$ through a similarity transformation. Equation (19) can then be rewritten as

$$\mathrm{E}[\mathbf{Q}^{\mathrm{T}}\mathbf{v}(k+1)] = \left[\mathbf{I}-\frac{\mu\mathbf{Q}^{\mathrm{T}}\mathbf{R}}{N\sigma_s^2}\right]\mathrm{E}[\mathbf{v}(k)] - \alpha_1\mathbf{Q}^{\mathrm{T}}\mathrm{E}\left[\frac{\mathrm{sgn}(\hat{\mathbf{h}}(k))}{|\hat{\mathbf{h}}(k-1)|+\varepsilon_1}\right], \tag{21}$$

so,

$$\begin{aligned}\mathbf{g}(k) &= \mathbf{Q}^{\mathrm{T}}\mathbf{v}(k);\\ \mathbf{h}'(k) &= \alpha_1\mathbf{Q}^{\mathrm{T}}\mathrm{E}\left[\frac{\mathrm{sgn}(\hat{\mathbf{h}}(k))}{|\hat{\mathbf{h}}(k-1)|+\varepsilon_1}\right].\end{aligned} \tag{22}$$

Let $\mathbf{q}$ be the sum of the absolute value of the ith element of $\mathbf{Q}^{\mathrm{T}}$. Thus, $\mathbf{h}'(k)$ is bounded between the diagonal element of $-(\alpha_1 q_m/\varepsilon_1)\mathbf{I}$ and $(\alpha_1 q_m/\varepsilon_1)\mathbf{I}$, so (21) can be written as

$$\mathrm{E}[\mathbf{g}(k+1)] = \left[\mathbf{I}-\frac{\mu\mathbf{\Lambda}}{N\sigma_s^2}\right]\mathrm{E}[\mathbf{g}(k)] - \mathbf{h}'(k). \tag{23}$$

In the limit $k\to\infty$, $\mathrm{E}[\mathbf{g}(k)]$ remains constrained when $\left[\mathbf{I}-(\mu\mathbf{\Lambda}/N\sigma_s^2)\right]<1$, which is satisfied by $0<\mu<N(\sigma_s^2/\lambda_{\max})$. Here, $\lambda_{\max}$ shows the maximum eigenvalue of the correlation matrix $\boldsymbol{s}(k)$. The condition is satisfied with the mean convergence, which is the same result as with the standard NLMS algorithm.

3.2 | Excess MSE

From the above discussion, we can assume that the coefficients of the adaptive filter converge to their optimum values, but this is not the case in practice. Although the average coefficient vector converges to $\mathbf{g}(k)$, the immediate deviation from (4) produces EMSE due to the noisy gradient estimates.

In the steady state, if $\mathbf{n}(k)$ and $\boldsymbol{\nu}(k)$ are independent of $\mathbf{s}(k)$, we can use the orthogonality principle and the fact that the AWGN has zero mean. The Gaussian input sequences $\mathrm{E}[\mathbf{s}(k)\mathbf{s}^{\mathrm{T}}(k)\mathbf{v}(k)\mathbf{v}^{\mathrm{T}}(k)\mathbf{s}(k)\mathbf{s}^{\mathrm{T}}(k)] = \mathbf{R}\mathrm{E}[\mathbf{v}(k)\mathbf{v}^{\mathrm{T}}(k)\mathbf{R}+\mathbf{R}\mathrm{tr}\{\mathbf{R}\mathrm{E}[\mathbf{v}(k)\mathbf{v}^{\mathrm{T}}(k)]\}$, as derived by [36]. By using (15), the mean value of $\mathbf{v}(k+1)\mathbf{v}^{\mathrm{T}}(k+1)$ is

$$\begin{aligned}\mathrm{E}[\mathbf{v}(k+1)\mathbf{v}^{\mathrm{T}}(k+1)] &= \mathrm{E}[\mathbf{v}(k)\mathbf{v}^{\mathrm{T}}(k)] + \frac{\mu^2}{\chi^2}\sigma_s^2\mathbf{R}\\ &-\frac{\mu}{\chi}\left(\mathrm{E}[\mathbf{v}(k)\mathbf{v}^{\mathrm{T}}(k)]\mathbf{R}+\mathbf{R}\mathrm{E}[\mathbf{v}(k)\mathbf{v}^{\mathrm{T}}(k)]\right)\\ &+\frac{\mu^2}{\chi^2}\left(2\mathbf{R}\mathrm{E}[\mathbf{v}(k)\mathbf{v}^{\mathrm{T}}(k)]\mathbf{R}+\mathbf{R}\mathrm{tr}\{\mathbf{R}\mathrm{E}[\mathbf{v}(k)\mathbf{v}^{\mathrm{T}}(k)]\}\right)\\ &-\frac{\mathbf{y}(k)}{\chi}+\mathbf{z}(k),\end{aligned} \tag{24}$$

where $\chi = N\sigma_s^2+\delta$, and

$$\mathbf{y}(k) = \alpha_1\left((\mathbf{I}-\mu\mathbf{R})\mathrm{E}\left[\mathbf{v}(k)\frac{\mathrm{sgn}(\mathbf{h}^{\mathrm{T}}(k))}{(|\mathbf{h}^{\mathrm{T}}(k-1)|+\varepsilon_1)}\right] + \mathrm{E}\left[\frac{\mathrm{sgn}(\mathbf{h}(k))}{(|\mathbf{h}(k-1)|+\varepsilon_1)}\mathbf{v}^{\mathrm{T}}(k)\right](\mathbf{I}-\mu\mathbf{R})\right), \tag{25}$$

$$\mathbf{z}(k) = \alpha_1^2\mathrm{E}\left[\frac{\mathrm{sgn}(\mathbf{h}(k))}{(|\mathbf{h}(k-1)|+\varepsilon_1)}\frac{\mathrm{sgn}(\mathbf{h}^{\mathrm{T}}(k))}{(|\mathbf{h}^{\mathrm{T}}(k-1)|+\varepsilon_1)}\right]. \tag{26}$$

In the limit $k\to\infty$, the correlation vector of mean coefficient error in (24) is $\mathrm{E}[\mathbf{v}(k)\mathbf{v}^{\mathrm{T}}(k)] = \mathbf{R}(v)$, which gives

$$\mathbf{R}(v)=\mathbf{R}(v)-\frac{\mu}{\chi}(\mathbf{R}(v)\mathbf{R}+\mathbf{R}\mathbf{R}(v)])+\frac{\mu^2}{\chi^2}\sigma_s^2\mathbf{R}+\frac{\mu^2}{\chi^2}(2\mathbf{R}\mathbf{R}(v)\mathbf{R}+\mathbf{R}\mathrm{tr}\{\mathbf{R}\mathbf{R}(v)\})+\lim_{k\to\infty}\left(\mathbf{z}(k)-\frac{\mathbf{y}(k)}{\chi}\right). \tag{27}$$

In the next step, note that $\sigma_n^2+\mathrm{tr}\{\mathbf{R}\mathbf{R}(v)\}$ is a scalar quantity. Taking the trace and multiplying $(\mathbf{I}-\mu\mathbf{R})^{-1}$ on both sides of (24), we obtain

$$\frac{1}{\chi}\left(\mathrm{tr}\{\mathbf{R}\mathbf{R}(v)\}+\mathrm{tr}\{(\mathbf{I}-\mu\mathbf{R})\mathbf{R}(v)\mathbf{R}(\mathbf{I}-\mu\mathbf{R})^{-1}\}\right)=\frac{\mu}{\chi}\left(\sigma_n^2+\mathrm{tr}\{\mathbf{R}\mathbf{R}(v)\}\right)\mathrm{tr}\{\mathbf{R}(\mathbf{I}-\mu\mathbf{R})^{-1}\}+\frac{1}{\mu}\lim_{k\to\infty}\left[\left(\mathbf{z}(k)-\frac{\mathbf{y}(k)}{\chi}\right)(\mathbf{I}-\mu\mathbf{R})^{-1}\right]. \tag{28}$$

On the basis of the properties of a trace, we obtain $\mathrm{tr}\{(\mathbf{I}-\mu\mathbf{R})\mathbf{R}(v)\mathbf{R}(\mathbf{I}-\mu\mathbf{R})^{-1}\}$ equal $\mathrm{tr}\{\mathbf{R}(v)\mathbf{R}(\mathbf{I}-\mu\mathbf{R})(\mathbf{I}-\mu\mathbf{R})^{-1}\}$, which is equal to $\mathrm{tr}\{\mathbf{R}(v)\mathbf{R}\}$, where $(\mathbf{I}-\mu\mathbf{R})$ is a symmetric matrix. The EMSE $\xi=\mathrm{tr}\{\mathbf{R}\mathbf{R}(v)\}$ is

$$\xi=\frac{\mu\mathrm{tr}\{\mathbf{R}(\mathbf{I}-\mu\mathbf{R})^{-1}\}}{2-\mu\mathrm{tr}\{\mathbf{R}(\mathbf{I}-\mu\mathbf{R})^{-1}\}}\sigma_n^2+\frac{\lim_{k\to\infty}\left((\chi\mathbf{z}(k)-\mathbf{y}(k))(\mathbf{I}-\mu\mathbf{R})^{-1}\right)}{\mu\left(2-\mu\mathrm{tr}\{\mathbf{R}(\mathbf{I}-\mu\mathbf{R})^{-1}\}\right)}. \tag{29}$$

Now $\mathbf{y}(k)$ and $\mathbf{z}(k)$ are being observed. Let $\mathbf{A}(k)$ and $\mathbf{B}(k)$ be written as $\mathrm{tr}\{\mathbf{y}(k)(\mathbf{I}-\mu\mathbf{R})^{-1}\}$ and $\mathrm{tr}\{\mathbf{z}(k)(\mathbf{I}-\mu\mathbf{R})^{-1}\}$, respectively, where $(\mathbf{I}-\mu\mathbf{R})^{-1}=\mathbf{Q}\Lambda^{-1}\mathbf{Q}^{\mathrm{T}}$, because of the eigenvalue, which is decomposed into $\mathbf{R}$ and $\mathbf{Q}$, which are orthogonal matrices. So, $\mathbf{B}(k)$ can be defined as

$$\mathbf{B}(k)\equiv\alpha_1^2\left(\mathrm{E}\left[\mathrm{tr}\left\{\Lambda^{-1}\mathbf{Q}^{\mathrm{T}}\frac{\mathrm{sgn}(\mathbf{h}(k))}{(|\mathbf{h}(k-1)|+\varepsilon_1)}\frac{\mathrm{sgn}(\mathbf{h}^{\mathrm{T}}(k))}{(|\mathbf{h}^{\mathrm{T}}(k-1)|+\varepsilon_1)}\mathbf{Q}\right\}\right]\right). \tag{30}$$

Let μ be a small step such that $(1-\mu\lambda_{\max})^{-1}$ is nonnegative. Equation (30) infers $\Lambda^{-1}\le(1-\mu\lambda_{\max})^{-1}$, so

$$\mathbf{B}(k)\le\frac{\alpha_1^2}{1-\mu\lambda_{\max}}\left(\mathrm{E}\left[\mathrm{tr}\left\{\mathbf{Q}^{\mathrm{T}}\frac{\mathrm{sgn}(\mathbf{h}(k))}{(|\mathbf{h}(k-1)|+\varepsilon_1)}\frac{\mathrm{sgn}(\mathbf{h}^{\mathrm{T}}(k))}{(|\mathbf{h}^{\mathrm{T}}(k-1)|+\varepsilon_1)}\mathbf{Q}\right\}\right]\right). \tag{31}$$

Equation (31) can be written as

$$\mathbf{B}(k)\le\frac{N\alpha_1^2}{\varepsilon_1^2(1-\mu\lambda_{\max})}. \tag{32}$$

Let us define $\mathcal{L}(k)\equiv\Lambda^{-\frac{1}{2}}\mathbf{Q}^{\mathrm{T}}\mathrm{sgn}(\mathbf{h}(k))/(|\mathbf{h}(k-1)|+\varepsilon_1)$. Moreover, $\mathbf{B}(k)$ in (30) can also be written as

$$\mathbf{B}(k)=\alpha_1^2\mathrm{E}(\|\mathcal{L}(k)\|_2^2), \tag{33}$$

where $\|(\bullet)\|_2^2$ is represented as an l_2-norm. Therefore, in (33), $\mathbf{B}(k)$ is a positive value. Now the variable $\mathbf{A}(k)$ is defined as

$$\mathbf{A}(k)\equiv 2\alpha_1\left(\mathrm{E}\left[\mathrm{tr}\left\{\mathbf{h}(k)\frac{\mathrm{sgn}(\mathbf{h}^{\mathrm{T}}(k))}{(|\mathbf{h}^{\mathrm{T}}(k-1)|+\varepsilon_1)}\right\}\right]-\mathrm{E}\left[\mathrm{tr}\left\{\mathbf{h}^{\mathrm{T}}(k)\frac{\mathrm{sgn}(\mathbf{h}(k))}{(|\mathbf{h}(k-1)|+\varepsilon_1)}\right\}\right]\right). \tag{34}$$

The common assumption from Chen and others [15] explains that $\lim_{k\to\infty}E[\mathrm{sgn}(\boldsymbol{h}(k))]=\mathrm{sgn}(\boldsymbol{h}(k))$, so (34) can be rewritten as

$$\mathbf{A}(k)=2\alpha_1\left(\mathrm{E}\left[\left\|\frac{\mathbf{h}(k)}{(|\mathbf{h}(k-1)|+\varepsilon_1)}\right\|_1\right]-\mathrm{E}\left[\left\|\frac{\mathbf{h}}{(|\boldsymbol{h}(k-1)|+\varepsilon_1)}\right\|_1\right]\right). \tag{35}$$

Defining $\Theta\triangleq[\lim_{k\to\infty}(\mathrm{tr}\{\mathbf{z}(k)(\mathbf{I}-\mu\mathbf{R})^{-1}\})]/\alpha_1^2$ and $\omega\equiv[\lim_{k\to\infty}(\mathrm{tr}\{\mathbf{y}(k)(\mathbf{I}-\mu\mathbf{R})^{-1}]/\})\alpha_1$, the EMSE from (29) can be rewritten as

$$\xi=\frac{\kappa}{2-\kappa}\sigma_n^2+\frac{\Theta\chi\alpha_1}{\mu(2-\kappa)}\left(\alpha_1-\frac{\omega}{\chi\Theta}\right), \tag{36}$$

where $\kappa=\mu\mathrm{tr}\{\mathbf{R}(\mathbf{I}-\mu\mathbf{R})^{-1}\}$ and Θ is nonnegative. If ω is defined as a positive integer, then the reweighted l_1-norm coefficient $\alpha_1<\omega/\chi\Theta$, which can be compared with the standard NLMS and RLMS, shows that the AZA-RNLMS algorithm performs better than the standard NLMS algorithm. In (36), ω varies according to the expected CIR sparsity standard.

Furthermore, the simulation results based on (36) for the AZA-RNLMS algorithm indicate an EMSE that is smaller than that of the standard NLMS and RLMS algorithm, such that a relatively low sparsity level is required for $\mathbf{A}(k)>0$. Using the underwater sparse channel followed by the i.i.d. Gaussian sparse channel, the simulation results are used to demonstrate the different levels of comparison of the NLMS algorithms and RLMS with the proposed AZA-RNLMS algorithm.

4 | SIMULATION AND EXPERIMENTS FOR UNDERWATER ACOUSTIC CHANNEL ESTIMATES

Computer simulations have been carried out to evaluate the performance of the proposed algorithm with respect to the efficiency of the sparsity-aware algorithms in stationary scenarios. The standard NLMS [8, 9], ZA-NLMS

[37], RZA-NLMS [24], RLMS [16], RLNMAT [27], and SNLMS [28] have been simulated and compared with the proposed AZA-RNLMS algorithm. The oracle NLMS is used to introduce the lower bound for all sparse-aware NLMS algorithms. Assumptions are made in the oracle NLMS algorithm that the sparse channel taps of nonzero position are known a priori. Two experiments have been performed: First, each nonzero CIR is chosen as a Gaussian random variable with zero mean and unity variance [38], and second, the underwater CIR is used. We considered a stationary device detection scenario for validating the empirical concepts in the mean behavioral study. The unknown system weight coefficients $\mathbf{h}(k)$ have been generated to ensure that the entire network has a sparse structure. Specifically, the CIR of the sparse system is that of an underwater channel between a hydrophone and a corresponding underwater speaker that is evaluated in real-time. It is a typical CIR for numerous practical system identification problems involving a particular degree of sparsity. Table 1 compares the different estimated-weight adaptive algorithms with the proposed AZA-RNLMS algorithm. In all experimental scenarios, the adaptive filter coefficients are all initialized to zero.

4.1 | I.I.D. Gaussian channel

The i.i.d. Gaussian channel [38] is generated randomly with CIR having zero mean and unity variance. In the first experiment, the unknown sparse system has 10 taps CIR with only 1 nonzero tap, so the degree of sparsity is 1/10 and is set to 1 or −1 with the same probabilities (each equal to 1/2). Further experiments for degrees of sparsity 40/100 and 20/100 have been performed.

Figure 2 compares the MSE performance with the regular NLMS [8, 9], ZA-NLMS [37], RZA-NLMS[24], RNLMAT[27], SNLMS[28], and RLMS[16] at 10 and 20 dB SNR. The degree of sparsity is 1/10. A Gaussian distribution with zero mean and unit variance selects the values of numerous large coefficients. The step index $\mu = 1$ and $\delta = 0.005$ are used for all NLMS algorithms. The rest of the parameters are set for RLMS, where $\alpha_r = 1.5 \times 10^{-4}$ is assigned to the l_1 minimization constant, and $\varepsilon_1 = 0.5$. The other parameters are $\alpha_{ZA} = \alpha_{RZA} = 5 \times 10^{-4}$ and $\varepsilon_1 = 10$.

Figure 2 shows that the AZA-RNLMS algorithm performs better than other algorithms and has a better convergence rate than the others. For a given degree of sparsity, the convergence is faster at 20 dB SNR than at 10 dB SNR. At SNRs of 20 dB and 10 dB, after 100 iterations, the proposed AZA-RNLMS algorithm converges and produces that are 26 dB and 37 dB better than the MSE, respectively, which is advantageous when the degree of sparsity is 1/10. Plotting the MSE from (14) shows that the AZA-RNLMS algorithm produces better steady-state performance and faster convergence than the conventional NLMS and RLMS algorithms.

Figures 3 and 4 compare the MSE performance of six traditional approaches, standard NLMS, ZA-NLMS, RZA-NLMS, RNLMAT, SNLM, and RLMS, to evaluate the proposed scheme. In this experiment, μ is set to unity, and the remaining parameters are the same as in the previous experiment. Figures 3 and 4 make the comparison for a degree of sparsity of 20/100 and 40/100, respectively. The

TABLE 1 Comparisons of the various algorithms

Algorithms	Estimated weight equation
NLMS [8, 9]	$\hat{\mathbf{h}}(k+1) = \hat{\mathbf{h}}(k) + \mu(k)\mathbf{e}(k)\mathbf{s}(k)$
ZA-NLMS [37]	$\hat{\mathbf{h}}(k+1) = \hat{\mathbf{h}}(k) + \frac{\mu \mathbf{e}(k)\mathbf{s}(k)}{\mathbf{s}^T(k)\mathbf{s}(k)+\delta} - \alpha_{ZA}\mathrm{sgn}(\hat{\mathbf{h}}(k))$
RZA-NLMS [24]	$\hat{\mathbf{h}}(k+1) = \hat{\mathbf{h}}(k) + \mu\frac{\mathbf{e}(k)\mathbf{s}(k)}{\mathbf{s}^T(k)\mathbf{s}(k)+\delta} - \alpha_{RZA}\frac{\mathrm{sgn}(\hat{\mathbf{h}}(k))}{\lvert\hat{\mathbf{h}}(k)\rvert+\varepsilon_{RZA}}$
RLMS [16]	$\hat{\mathbf{h}}(k+1) = \hat{\mathbf{h}}(k) + \mu\mathbf{e}(k)\mathbf{s}(k) - \alpha_r\frac{\mathrm{sgn}(\hat{\mathbf{h}}(k))}{\lvert\hat{\mathbf{h}}(k-1)\rvert+\varepsilon_1}$
RNLMAT [27]	$\hat{\mathbf{h}}(k+1) = \hat{\mathbf{h}}(k) + \mu\frac{\mathrm{sgn}[\mathbf{e}(k)]\mathbf{s}(k)}{\mathbf{s}^T(k)\mathbf{s}(k)+\delta}\min\{e^2(k), e_{up}\} - \alpha_r\frac{\mathrm{sgn}(\hat{\mathbf{h}}(k-1))}{\lvert\hat{\mathbf{h}}(k)\rvert+\varepsilon_{RZA}}$
SNLMS[a] [28]	$\hat{\mathbf{h}}(k+1) = \hat{\mathbf{h}}(k) + \mu\frac{\mathbf{W}(k)\mathbf{s}(k)\mathbf{e}(k)}{\mathbf{s}^T(k)\mathbf{W}(k)\mathbf{s}(k)+\delta} - g(h_i)$
Proposed algorithm	$\hat{\mathbf{h}}(k+1) = \hat{\mathbf{h}}(k) + \mu\frac{\mathbf{e}(k)\mathbf{s}(k)}{\mathbf{s}^T(k)\mathbf{s}(k)+\delta} - \alpha_{ar}(k+1)\frac{\mathrm{sgn}(\hat{\mathbf{h}}(k))}{\lvert\hat{\mathbf{h}}(k-1)\rvert+\varepsilon_1}$

[a]To use the SNLMS algorithms that encourage sparsity without introducing bias into the adaptation process by using the regularization coefficient $\gamma_1 = 0$, where $\mathbf{W}(k) = M\beta^2(k)/\mathrm{tr}\{\beta^2(k)\}$ [28], and for the l_1 reweighted framework, the log-sum penalty with $g(h_i) = \log(|\hat{\mathbf{h}}(k)| + \varepsilon_1), \varepsilon_1 > 0$ [10, 28]. Note that from, Equation (28), we always have $\mathrm{tr}\{\mathbf{W}(k)\} = M$ [28], which is aligned with the non-affine scaling transformation case and basically has $\mathbf{W}(k) = \mathbf{I}$, whose trace is also M.

Abbreviations: NLMS, normalized least-mean-squares; RLMS, reweighted least-mean-square; RNLMAT, reweighted normalized least mean absolute third; RZA-NLMS, reweighted zero-attracting-normalized least-mean-squares; SNLMS, sparsity-promoting normalized least-mean-squares.

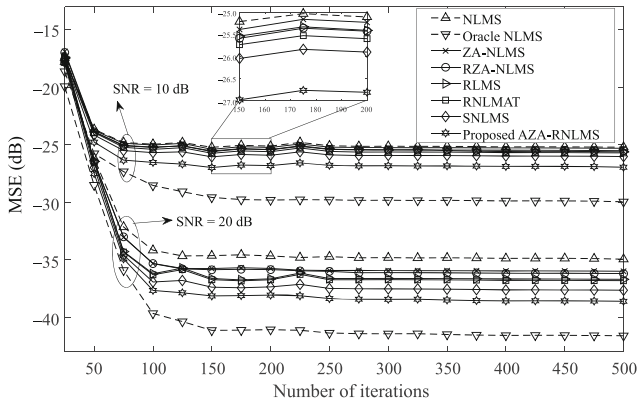

FIGURE 2 Learning curve (mean-square-errors [MSEs]) of sparsity-aware estimation algorithms, where the degree of sparsity is 1/10

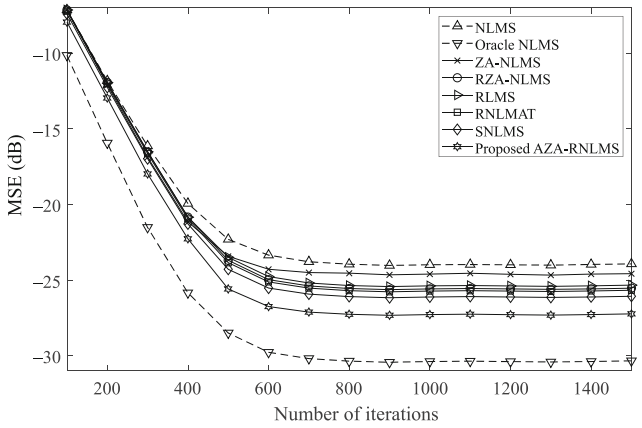

FIGURE 3 Learning curve (mean-square-errors [MSEs]) of sparsity-aware estimation algorithms, where the degree of sparsity is 40/100 and $\mu = 1$

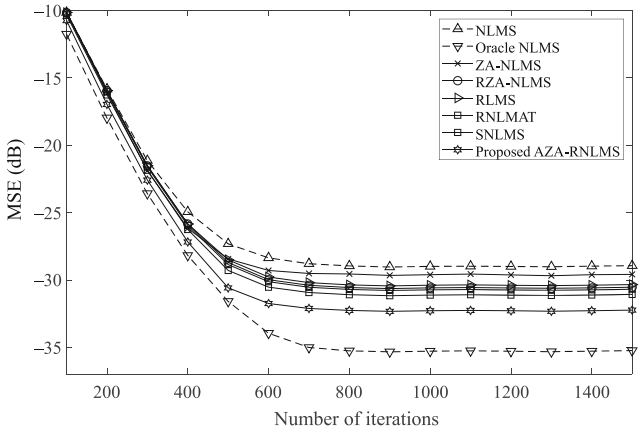

FIGURE 4 Learning curve (mean-square-errors [MSEs]) of sparsity-aware estimation algorithms, where the degree of sparsity is 20/100 and $\mu = 1$

proposed AZA-RNLMS algorithm converges at 700 iterations, and the ZA-NLMS algorithm converges at 600 iterations, but the MSE at a degree of sparsity of 40/100 and 20/100 is 9.76% and 8.55%, respectively, less than that of the proposed AZA-RNLMS. Of course, the accuracy of the channel estimate would improve under the same sparsity with a longer channel length, but the purpose of this experiment is to demonstrate faster convergence for a higher degree of sparsity. The results show that the MSE improves with decreasing sparsity, which is highly desirable for the high-sparsity channel.

Furthermore, Table 2 compares the proposed AZA-RNLMS scheme with the conventional algorithms (the proposed scheme has the lowest MSE). In addition, while the sparse-channel estimation is more accurate for channels with a high degree of sparsity, the accuracy decreases significantly if the channel becomes non-sparse, as is common in real-world communication environments.

Figures 5 and 6 show the effectiveness of the proposed system and compare it with the MSE performance of six conventional algorithms: regular NLMS, ZA-NLMS, RZA-NLMS, RNLMAT, SNLMS, and RLMS. For the large-sparsity CIR, the degree of sparsity in Figures 5 and 6 is set to 40/100 and 20/100, respectively. In Figures 5 and 6, the proposed AZA-RNLMS algorithm converges after 1000 iterations and produces a MSE lower than -31 dB and -35 dB, respectively. Similarly, reweighted NLMS algorithms and the RLMS algorithm also converge at around 1000 iterations, with the exception being the standard NLMS algorithm. The NLMS converges at about 900 iterations, but the MSE for sparsities of 40/100 and 20/100 are 27.13% and 27.70%, respectively, lower than the that of the proposed AZA-RNLMS algorithm. Table 2 compares the converged MSEs from Figures 3–6.

The proposed AZA-RNLMS algorithm is better than the conventional NLMS algorithms at different SNRs and converges faster for a high-sparsity channel because sparse AZA-RNLMS algorithms use the l_1-norm, which reflects the adaptivity of the iteration to estimate error. In other words, the AZA-RNLMS algorithm for an extremely sparse channel uses a large step size to accelerate convergence but uses a small size to increase the precision of the estimate for a low-sparsity channel. Table 2 compares the various sparsity-aware algorithms in terms of MSE for a Gaussian channel.

Figure 7 shows the MSE for all sparse-aware NLMS algorithms for various degrees of system sparsity. The proposed AZA-RNLMS algorithm outperforms all other sparse-aware NLMS algorithms. Although we have assumed a sparse channel, this is not recommended for actual propagation channels because the degree of channel sparsity is not stable, and a sparse channel may become non-sparse. The performance of a sparse-channel

TABLE 2 Comparison table for MSE convergence using Gaussian channel

	MSE (dB)			
	Step value ($\mu = 0.5$)		Step value ($\mu = 1$)	
Algorithms	Degree of sparsity (40/100)	Degree of sparsity (20/100)	Degree of sparsity (40/100)	Degree of sparsity (20/100)
NLMS	−23.4	−26.7	−24.01	−29.1
ZA-NLMS	−28.7	−31.7	−24.7	−29.6
RZA-NLMS	−30.6	−35.4	−25.6	−30.6
RLMS	−30.3	−33.7	−25.4	−30.4
RNLMAT	−30.8	−35.5	−25.8	−30.8
SNLMS	−31.2	−35.9	−26.2	−31.2
Proposed algorithm	−32.1	−36.9	−27.3	−32.3

Abbreviations: MSE, mean-square-error; NLMS, normalized least-mean-squares; RLMS, reweighted least-mean-square; RNLMAT, reweighted normalized least mean absolute third; RZA-NLMS, reweighted zero-attracting-normalized least-mean-squares; SNLMS, sparsity-promoting normalized least-mean-squares; ZA-NLMS, zero-attracting-normalized least-mean-squares.

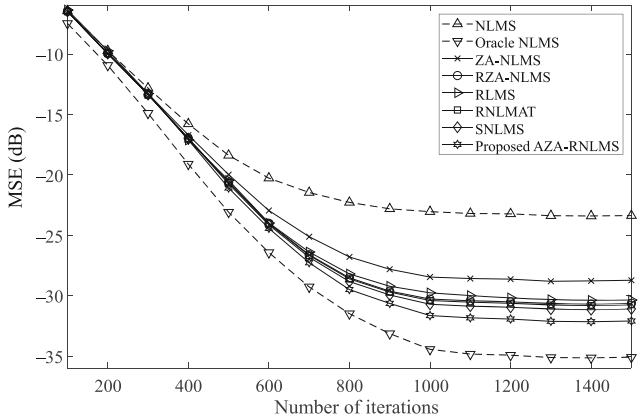

FIGURE 5 Learning curve (mean-square-errors [MSEs]) of sparsity-aware estimation algorithms, where the degree of sparsity is 40/100 and $\mu = 0.5$

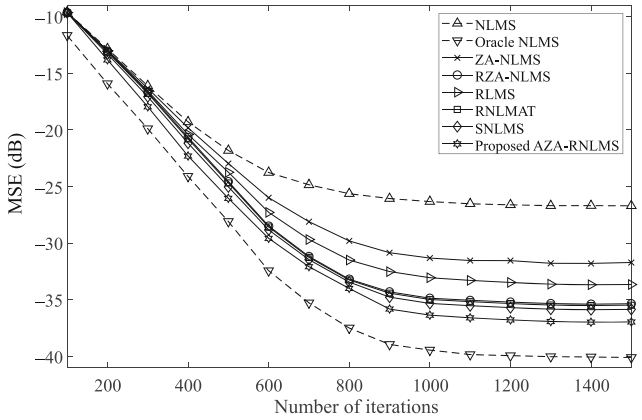

FIGURE 6 Learning curve (mean-square-errors [MSEs]) of sparsity-aware estimation algorithms, where the degree of sparsity is 20/100 and $\mu = 0.5$

estimator will degrade significantly in this situation. The performance of the SNLMS algorithm decreases to that of the RNLMAT algorithm when the degree of sparsity approaches 60/100. Similarly, the performance of the RNLMAT algorithm decreases to that of the RZA-NLMS algorithm below 40/100. The maximum channel delay is defined directly by the degree of sparsity. In other words, the uncertainty principle, which dictates the localization of the nonstationary channel delay spread, should be extended to account for the fluctuating sparseness of the channel. When using more dimensions of signal space, the sparsity increases compared with the scenario in which all the multipath components are distributed only in the delay domain.

Figure 8 shows the learning curve for EMSE (i.e., the EMSE as a function of the number of iterations). The AZA-RNLMS algorithm is compared with the standard NLMS algorithm and RLMS algorithm [16] for a CIR length of 100, and the degree of sparsity is varied over 10/100, 20/100, 30/100, 40/100. The regular NLMS algorithm produces the same EMSE, irrespective of CIR or the degree of sparsity. The nonzero CIR taps are selected at random, with nonzero taps set to 1 or −1 with a probability of 0.5. The parameters for the RLMS algorithms are defined as $\alpha_r = 1.5 \times 10^{-4}$ and $\varepsilon_1 = 0.05$. To increase the convergence speed, the step size $\mu = 0.5$. The noise variance σ_n^2 is set to unity for the AWGN algorithm so that the regular NLMS algorithms have the same EMSE, irrespective of channel sparsity. The EMSE for the AZA-RNLMS algorithm is calculated from (5) as $\xi(k) = \mathrm{tr}\{\mathbf{R}\mathbf{E}[\mathbf{v}(k)\mathbf{v}^{\mathrm{T}}(k)]\}$, where $\mathbf{s}(k)$ is an i.i.d. binary-phase-shift keying sequence. However, with increased sparsity, the EMSE of the AZA-RNLMS algorithm increases because of the decrease of $\mathbf{A}(k)$ in (35). The

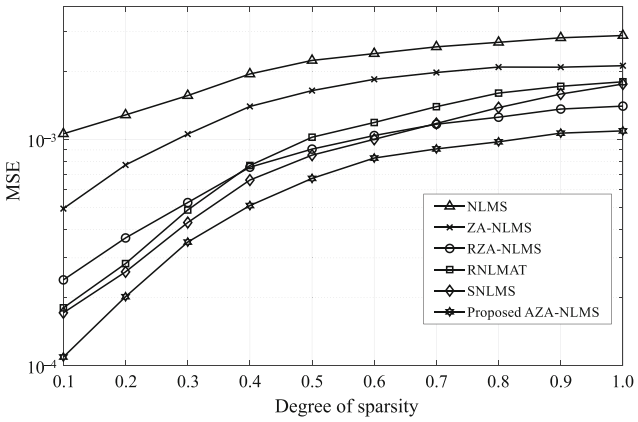

FIGURE 7 Performance of mean-square-error (MSE) of proposed adaptive zero-attracting-reweighted normalized least-mean-square (AZA-RNLMS), sparsity-promoting normalized least-mean-squares (SNLMS), reweighted normalized least mean absolute third (RNLMAT), reweighted zero-attracting-normalized least-mean-squares (RZA-NLMS), ZA-NLMS, and NLMS with varying system sparsity and 100 maximum channel taps. The signal-to-noise ratio (SNR) and μ are set to 20 dB and 1, respectively

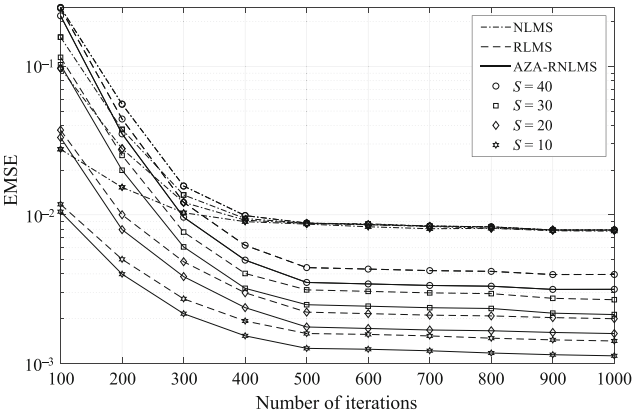

FIGURE 8 Learning curve for excess mean-square-error (EMSE) at various sparsity

AZA-RNLMS algorithm thus outperforms the regular NLMS algorithm and RLMS algorithm under all conditions.

4.2 | Simulated underwater SPACE08 channel

We use the channel gain obtained from the SPACE08 experiment, which was done off the shore of Martha's Vineyard, USA in the fall of 2008 to measure the efficiency of adaptive power and the rate control of an acoustic channel. This experiment transmitted repeatedly a pseudo-random channel sampling sequence of length 4095,

TABLE 3 Parameters for underwater channel system

Parameters	SPACE08
Transmitter depth (m)	4
Receiver depth (m)	2
Bandwidth (kHz)	9
Carrier frequency (kHz)	13
Minimum frequency (kHz)	8.5
Roll-off factor	0.38
Time resolution (ms)	50
Frequency resolution (Hz)	25
Relative velocity (between Tx and Rx) (m/s)	0
Spreading factor	1.7
Channel length (km)	1

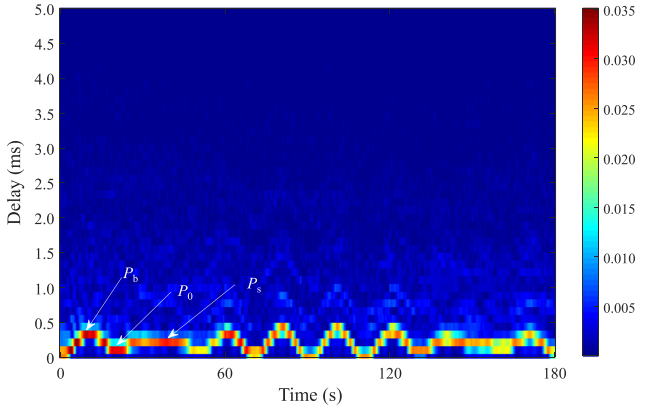

FIGURE 9 Two-dimensional diagram of underwater acoustics channel impulse response (CIR)

modulated on a 12.5 kHz carrier using a binary-phase-shift keying sequence. The channel parameters for the simulation were taken from previous studies [1, 39, 40]. Certain channel parameters were slightly tuned to achieve a near correlation between measurement and simulation. The channel parameters appear in Table 3.

For the CIR of SPACE08, the first arrival is the direct arrival (P_0), closely accompanied by the surface (P_s) and the arrival (P_b) mirrored in the floor (see Figure 9). The successive arrivals are triggered by many interactions between the surface and the floor. Primary and secondary multipath reflections from the flowing ocean surface and static sea bottom cause a large spread in the time-varying delay in the UWA channel. The calculated information reveals a similarity between the arrival times of closely spaced iterations in some of the arrivals, which does not appear in the present simulation.

The correlation is needed because the channel changes slowly over time and is thus correlated over

short periods. The measured average arrival intensity is very close to that predicted. The simulation predicts that the direct and surface-reflected arrivals are slightly more faded than observed. The direct arrival of the acoustic waves from the transmitter to the receiving hydrophone reflects the line of sight. Because significant uncertainty is associated with the sparsity across the transient delay taps, sparsity-aware techniques are difficult to use directly in the shallow-water domain without making significant effort.

Figure 10 shows the MSE performance, which is also used to evaluate the efficiency of the proposed AZA-RNLMS scheme with the six standard approaches (i.e., the standard NLMS, ZA-NLMS, RZA-NLMS, RNLMAT, SNLMS, and RLMS algorithms) for the UWA channel. The RZA-NLMS, RNLMAT, SNLMS, and RLMS algorithms are introduced to estimate the underwater acoustic channel. The parameters $\mu = 0.5, \alpha_r = 1.5 \times 10^{-4}$, and $\varepsilon_1 = 0.05$ are used for the RLMS and NLMS algorithm. The additive noise is selected with zero mean and unity variance ($\sigma_n^2 = 1$). The ZA-NLMS and RZA-NLMS results are close to each other and are more accurate than the results of the standard NLMS algorithm. In addition, the l_1-norm reweighted RLMS, RNLMAT, and SNLMS algorithms produce much better results than do the ZA-NLMS and RZA-NLMS algorithms. For SNRs of 10 and 20 dB, all algorithms converge around 100 and 120 iterations, respectively. Table 4 compares the MSEs for the underwater channel.

The results given in Figure 10 and Table 4 prove that the AZA-RNLMS algorithm delivers better steady-state performance and convergence rate than the conventional NLMS and RLMS algorithms. Note that, for the same sparsity, the accuracy of the underwater-channel estimate would improve with a longer channel length. Therefore, for a larger underwater channel length, the proposed algorithm performs better.

Figure 11 shows the learning curve for the EMSE (i.e., the EMSE as a function of the number of iterations) for the UWA channel. The parameters for the AZA-RNLMS algorithm are $\alpha_r = 1.5 \times 10^{-4}$ and $\varepsilon_1 = 0.05$. The convergence is fast, and the step size $\mu = 0.5$. The standard NLMS algorithms have the same EMSE as the normalized AWGN algorithm, irrespective of channel sparsity. The EMSE for the proposed AZA-RNLMS algorithm is derived from (5). However, the EMSE of the AZA-RNLMS algorithm increases due to the reduction in $\mathbf{A}(k)$ with increasing sparsity (see 35). The proposed AZA-RNLMS algorithm thus performs better than the standard NLMS algorithm under all conditions.

TABLE 4 Comparison of MSE convergence for underwater channel

	MSE (dB)	
Algorithms	**SNR=10 dB**	**SNR=20 dB**
NLMS	−34.7	−44.6
ZA-NLMS	−35.9	−45.9
RZA-NLMS	−36.1	−45.9
RLMS	−37.1	−46.9
RNLMAT	−37.2	−47.02
SNLMS	−37.5	−47.4
Proposed algorithm	−38.4	−48.1

Abbreviations: MSE, mean-square-error; NLMS, normalized least-mean-squares; RLMS, reweighted least-mean-square; RNLMAT, reweighted normalized least mean absolute third; RZA-NLMS, reweighted zero-attracting-normalized least-mean-squares; SNLMS, sparsity-promoting normalized least-mean-squares; ZA-NLMS, zero-attracting-normalized least-mean-squares.

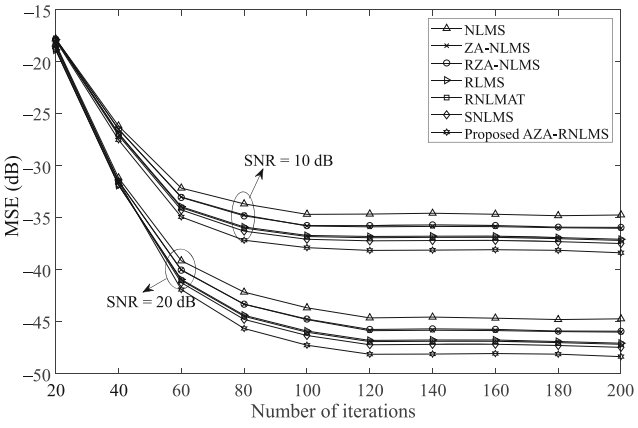

FIGURE 10 Learning curve (mean-square-errors [MSEs]) of sparsity-aware estimation algorithms for underwater acoustic channel

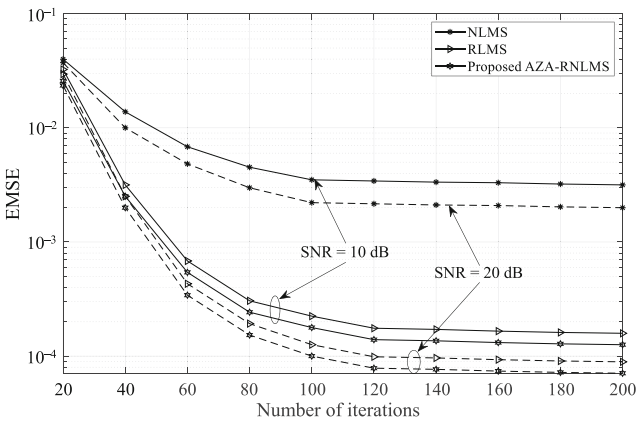

FIGURE 11 Learning curve of excess mean-square-error (MSE) for underwater acoustic channel

5 | CONCLUSIONS

This paper considers the problem of sparse direct-adaptive filtering channel estimation for underwater channels. The AZA-RNLMS algorithm is proposed, and its performance is evaluated. The AZA-RNLMS algorithm based on the adaptive l_1-norm minimization parameter algorithm is rigorously investigated based on the penalty term in the standard NLMS framework, resulting in faster convergence and greater accuracy for both Gaussian and underwater channels. A quantitative analysis for the AZA-RNLMS algorithm is presented, and the theoretical expressions for EMSE are derived. The simulation results show that the proposed adaptive convex-combination algorithm converges faster than the other sparsity-aware AZA-RNLMS algorithms and the conventional NLMS algorithms. The results for the EMSE demonstrate that, for large sparse CIR, the AZA-RNLMS algorithm outperforms the standard NLMS algorithm. The proposed AZA-RNLMS algorithm produces more accurate results than the conventional NLMS and RLMS algorithm for an underwater acoustic channel. The results of the AZA-RNLMS algorithm are compared with those of the ZA-NLMS, RZA-NLMS, RNLMAT, SNLMS, RLMS, and standard NLMS algorithms, where the MSE is approximately -36.9 dB and -48.1 dB in the Gaussian channel and simulated underwater channel, respectively. Performance evaluation with simulation as well as experimental data on acoustic channels has also been presented. The results obtained using the SPACE08 channel data clearly demonstrate the effectiveness of the proposed algorithm. The proposed channel estimation can thus be used to produce an efficient and reliable UWA communication system. An interesting extension of the present work would be to modify the AZA-RNLMS algorithm by integrating a variable step size.

ACKNOWLEDGMENT

The authors are grateful for the funding support of the Science and Engineering Research Board (SERB), Department of Science & Technology (DST), Government of India, vide file no. SRG/2020/002486.

CONFLICT OF INTEREST

The authors declare no conflicts of interest.

ORCID

Anand Kumar https://orcid.org/0000-0001-8724-2050
Prashant Kumar https://orcid.org/0000-0003-1017-2378

REFERENCES

1. P. Qarabaqi and M. Stojanovic, *Statistical characterization and computationally efficient modeling of a class of underwater acoustic communication channels*, IEEE J. Ocean. Eng. **38** (2013), no. 4, 701–717.
2. Y. Zhang, Y. V. Zakharov, and J. Li, *Soft-decision-driven sparse channel estimation and turbo equalization for MIMO underwater acoustic Communications*, IEEE Access **6** (2018), 4955–4973.
3. Y. Tian, X. Han, J. Yin, and Y. Li, *Adaption penalized complex LMS for sparse under-ice acoustic channel estimations*, IEEE Access **6** (2018), 63214–63222.
4. Z. Qin, J. Tao, and X. Han, *Sparse direct adaptive equalization based on proportionate recursive least squares algorithm for multiple-input multiple-output underwater acoustic communications*, J. Acous. Soc. Am. **148** (2020), no. 4, 2280–2287.
5. P. Kumar, V. K. Trivedi, and P. Kumar, *Recent trends in multicarrier underwater acoustic communications*, (IEEE Underwater Technology, Chemmai, India), Feb. 2015, pp. 1–8.
6. L. Liu, D. Sun, and Y. Zhang, *A family of sparse group Lasso RLS algorithms with adaptive regularization parameters for adaptive decision feedback equalizer in the underwater acoustic communication system*, Phys. Commun. **23** (2017), 114–124.
7. K. Pelekanakis and M. Chitre, *Comparison of sparse adaptive filters for underwater acoustic channel equalization/estimation*, (IEEE International Conference on Communication Systems, Singapore), Nov. 2010, pp. 395–399.
8. S. Haykin, *Adaptive filter theory*, Pearson Education, 2014.
9. B. Widrow and S. D. Stearns, *Adaptive signal processing*, Pearson, India, 2016.
10. E. J. Candès, M. B. Wakin, and S. P. Boyd, *Enhancing sparsity by reweighted l_1 minimization*, J. Fourier Anal. Appl. **14** (2008), no. 5-6, 877–905.
11. D. L. Duttweiler, *Proportionate normalized least-mean-squares adaptation in echo cancelers*, IEEE Trans. Speech Audio Process. **8** (2000), no. 5, 508–518.
12. K. Kumar, R. Pandey, M. L. N. S. Karthik, S. S. Bhattacharjee, and N. V. George, *Robust and sparsity-aware adaptive filters: A Review*, Signal Process. **189** (2021). https://doi.org/10.1016/j.sigpro.2021.108276
13. S. S. Bhattacharjee, D. Ray, and N. V. George, *Adaptive modified versoria zero attraction least mean square algorithms*, IEEE Trans. Circ. Syst. II: Express Briefs **67** (2020), no. 12, 3602–3606.
14. M. N. S. Jahromi, M. S. Salman, A. Hocanin, and O. Kukrer, *Mean-square deviation analysis of the zero-attracting variable step-size LMS algorithm*, Signal, Image Video Process. **11** (2017r), no. 3, 533–540.
15. Y. Chen, Y. Gu, and A. O. Hero, *Sparse LMS for system identification*, (IEEE International Conference on Acoustics, Speech and Signal Processing, Taipei, Taiwan), 2009, pp. 3125–3128.
16. O. Taheri and S. A. Vorobyov, *Reweighted l1-norm penalized LMS for sparse channel estimation and its analysis*, Signal Process. **104** (2014), 70–79.
17. X. Cao, F. Tong, B. Li, and S. Zheng, *Experimental evaluation of norm constraint sparsity exploitation for shallow water acoustic communication*, Appl. Acoust. **180** (2021), 108111.

18. C. Wang, Y. Zhang, Y. Wei, and N. Li, *A new l0-LMS algorithm with adaptive zero attractor*, IEEE Commun. Lett. **19** (2015), no. 12, 2150–2153.
19. F. Y. Wu, Y. H. Zhou, F. Tong, and R. Kastner, *Simplified p-norm-like constraint LMS algorithm for efficient estimation of underwater acoustic channels*, J. Mar. Sci. Appl. **12** (2013), no. 2, 228–234.
20. Y. Tian, X. Han, J. Yin, H. Chen, and Q. Liu, *An improved least mean square/fourth direct adaptive equalizer for under-water acoustic communications in the Arctic*, Acta Oceanol. Sin. **39** (2020), no. 9, 133–139.
21. D. Kari, I. Marivani, F. Khan, M. O. Sayin, and S. S. Kozat, *Robust adaptive algorithms for underwater acoustic channel estimation and their performance analysis*, Digit. Signal Process. A Rev. J. **68** (2017), 57–68.
22. S. Zhou, N. Xiu, Y. Wang, L. Kong, and H. Qi, *A null-space-based weighted l_1 minimization approach to compressed sensing*, Inf. Infer. **5** (2016), no. 1, 76–102.
23. A. Al-Shabili, L. Weruaga, and S. Jimaa, *Adaptive sparsity tradeoff for ℓ_1-constraint NLMS algorithm*, (IEEE International Conference on Acoustics, Speech and Signal Processing, Shanghai, China), 2016, pp. 4707–4711.
24. Y. Li, Y. Wang, and T. Jiang, *Sparse-aware set-membership NLMS algorithms and their application for sparse channel estimation and echo cancelation*, AEU - Int. J. Electron. Commun. **70** (2016), no. 7, 895–902.
25. Y. Wang and Y. Li, *Sparse multipath channel estimation using norm combination constrained set-membership NLMS algorithms*, Wirel. Commun. Mob. Comput. **2017** (2017). https://doi.org/10.1155/2017/8140702
26. S. Zhang and J. Zhang, *Set-membership NLMS algorithm with robust error bound*, IEEE Trans. Circ. Syst. II: Express Briefs **61** (2014), no. 7, 536–540.
27. R. Pogula, T. K. Kumar, and F. Albu, *Robust sparse normalized LMAT algorithms for adaptive system identification under impulsive noise environments*, Circ. Syst. Signal Process. **38** (2019), no. 11, 5103–5134.
28. C. H. Lee, B. D. Rao, and H. Garudadri, *Proportionate adaptive filtering algorithms derived using an iterative reweighting framework*, IEEE/ACM Trans. Audio Speech Lang. Process. **29** (2021), 171–186.
29. K. Pelekanakis and M. Chitre, *New sparse adaptive algorithms based on the natural gradient and the L_0-norm*, IEEE J. Ocean. Eng. **38** (2013), no. 2, 323–332.
30. Z. Jin, Y. Li, and Y. Wang, *An enhanced set-membership PNLMS algorithm with a correntropy induced metric constraint for acoustic channel estimation*, Entropy **19** (2017), no. 6. https://doi.org/10.3390/e19060281
31. I. Hassani, M. Arezki, and A. Benallal, *A novel set membership fast NLMS algorithm for acoustic echo cancellation*, Appl. Acoust. **163** (2020). https://doi.org/10.1016/j.apacoust.2020.107210
32. Y. Li, Y. Wang, and L. Sun, *A flexible sparse set-membership NLMS algorithm for multi-path and acoustic echo channel estimations*, Appl. Acoust. **148** (2019), 390–398.
33. J. Lim, H. Pang, and K. Lee, *Time delay estimation based on log-sum and l p -norm penalized minor component analysis*, J. Acoust. Soc. Am. **143** (2018), no. 6, 3979–3984.
34. A. Kumar and P. Kumar, *Underwater acoustic channel estimation via basic-CS and modified-CS using 2-D frequency sampling*, (IEEE International Conference on Advanced Communication Technologies and Signal Processing), 2020, pp. 1–6.
35. O. Macchi, N. Bershad, and M. Mboup, *Steady-state superiority of lms over ls for time-varying line enhancer in noisy environment*, IEE Proc. F Radar Signal Process. **138** (1991), no. 4, 354–360.
36. L. Horowitz and K. Senne, *Performance advantage of complex LMS for controlling narrow-band adaptive arrays*, IEEE Trans. Acoust. Speech Signal Process. **29** (1981), no. 3.
37. Y. Li and M. Hamamura, *An improved proportionate normalized least-mean-square algorithm for broadband multipath channel estimation*, The Sci. World J. **2014** (2014), 1–9.
38. M. S. Ahmed, N. S. Mohd Shah, Y. Y. Al-Aboosi, M. S. M. Gismalla, M. F. L. Abdullah, Y. A. Jawhar, and M. Balfaqih, *Filter orthogonal frequency-division multiplexing scheme based on polar code in underwater acoustic communication with non-Gaussian distribution noise*, ETRI J. **43** (2021), no. 2, 184–196.
39. A. Kumar and P. Kumar, *Pilot-assisted maximum-likelihood estimation for underwater acoustic communication*, IEEE Int. Conf. Comput. Commun. Secur. **1** (2020), 5–10.
40. Y. Zhang, R. Venkatesan, O. A. Dobre, and C. Li, *Efficient estimation and prediction for sparse time-varying underwater acoustic channels*, IEEE J. Ocean. Eng. **45** (2020), no. 3, 1112–1125.

AUTHOR BIOGRAPHIES

Anand Kumar received a BE degree in Electronics and Communications Engineering from Visveswaraiah Technological University Belagavi, Karnataka, India in 2015 and his ME degree in Electronics and Communication Engineering from the Birla Institute of Technology Mesra, Jharkhand, India in 2019. He is currently working toward his PhD at the National Institute of Technology Jamshedpur, Jharkhand, India, where he is also serving as a Project Associate. His research interests lie in the areas of underwater acoustic communication and networking, channel estimation, and underwater target detection and localization.

Prashant Kumar received a BSc Engg in Electronics and Communication Engineering from Patna University, India in 2002 and a MTech in Telecom Engineering from NIT Durgapur, India in 2007, and a PhD from IIT Patna, India in 2016. He has published several peer-reviewed research papers in journals and conference proceedings. His area of research includes wireless communication, underwater sensor networks, device-to-device communication, and microscale energy harvesting. He has over 19 years of

experience in teaching at the undergraduate and post-graduate levels and is presently serving as an Assistant Professor in the Department of Electronics and Communication Engineering at NIT Jamshedpur, India. He is a Senior IEEE Member and a life member of IETE and ISTE New Delhi, India. He is the principal investigator of two sponsored research projects in the area of underwater communication.

How to cite this article: A. Kumar and P. Kumar, *An improved sparsity-aware normalized least-mean-square scheme for underwater communication*, ETRI Journal **45** (2023), 379–393. https://doi.org/10.4218/etrij.2022-0036